2022

Efficient Removal of Lead Ions from Aqueous Media Using Sustainable Sources on Marine Algae

Hannah Namkoong

Erik Biehler

Gon Namkoong
Old Dominion University, gnamkoon@odu.edu

Tarek M. Abdel-Fattah

Original Publication Citation

Namkoong, H., Biehler, E., Namkoong, G., & Abdel-Fattah, T. M. (2022). Efficient removal of lead ions from aqueous media using sustainable sources based on marine algae. *ACS Omega*, *7*(44), 39931-39937. https://doi.org/10.1021/acsomega.2c04322

ACS OMEGA

http://pubs.acs.org/journal/acsodf

Article

Efficient Removal of Lead Ions from Aqueous Media Using Sustainable Sources Based on Marine Algae

Hannah Namkoong, Erik Biehler, Gon Namkoong, and Tarek M. Abdel-Fattah*

Cite This: *ACS Omega* 2022, 7, 39931−39937

Read Online

ACCESS | Metrics & More | Article Recommendations | Supporting Information

ABSTRACT: The goal of this project is to explore a new method to efficiently remove Pb(II) ions from water by processing *Undaria pinnatifida* into immobilized beads using sodium alginate and calcium chloride. The resulting biosorbent was characterized by Fourier transform infrared spectroscopy (FTIR) and scanning electron microscopy coupled with energy-dispersive X-ray spectroscopy (SEM-EDS). Using immobilized *U. pinnatifida*, we investigated the effect of various factors on Pb(II) ion removal efficiency such as temperature, pH, ionic strength, time, and underlying biosorption mechanisms. For Pb(II) ion biosorption studies, Pb(II) ion biosorption data were obtained and analyzed using Langmuir and Freundlich adsorption models. It is found that the maximum Pb(II) ion adsorption capacity (X_m) of *U. pinnatifida* was estimated to be ∼5 times greater than that of activated carbon, indicating the superior Pb(II) ion removal capability of *U. pinnatifida* compared to activated carbon. In addition, a thermodynamic study indicates that biosorption processes are found to be endothermic and an increase in the Pb(II) ion solution temperature provides a more preferential reaction toward Pb(II) ion biosorption.

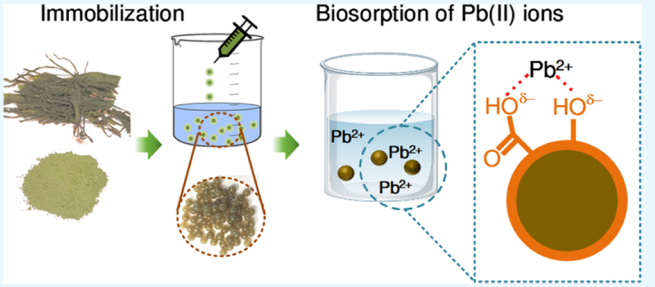

1. INTRODUCTION

In recent years, industrial development has led to a significant increase in the disposal of wastes containing different heavy metals in sewage or bodies of water. However, the high processing cost of industrial wastes increased the discharge of large amounts of potential hazardous heavy metals into the environment. Among many heavy metals, lead (Pb) is a highly toxic metal, causing a wide range of environmental contamination and health problems.[1] Lead sources are diverse, including many industrial plants, smoking, gasoline, paint, plumbing pipes, batteries, toys, faucets, car exhausts, etc.[2] Particularly, in the USA, more than 100 to 200 000 tons of lead are known to be emitted from car exhausts every year.[1] Unfortunately, some Pb(II) ions released into the environment can pose a risk to human health and can seriously damage aquatic life, plants, and animals.[3] In addition, Lo et al., reported that slight excess of lead (∼5 mg/mL) in drinking water can adversely affect health and cause high blood pressure, kidney damage, anemia, and others.[4] Hence, it is very important to remove lead from wastewater before it is released into an aquatic environment or directly consumed.

Much research has been conducted to remove Pb(II) ions from water.[5−13] For instance, Esalah et al. used sodium di-(*n*-octyl) phosphonate as a precipitating agent to remove Pb(II) ions from aqueous solutions.[5] Gupta et al. used red mud as an efficient adsorbent for the removal of lead from aqueous solutions.[6] Other conventional approaches for the removal of Pb(II) ions from wastewater include ion exchange, electroplating, chemical coagulation, membrane filtration, activated carbon, and advanced oxidation processes.[7,8] However, many of these conventional processes still involve high costs, high energy consumption, and large amounts of toxic waste.[9] Alternatively, a biological approach was considered a safer, cheaper, and more efficient method to eliminate heavy metals from water.[10] In particular, the use of algae has been extensively studied as a plausible way to remove Pb(II) ions from water, as it is abundant, relatively cheap to process, and can effectively remove high metal contents.[11−13] The biosorption of heavy metal ions by microorganisms has been investigated. First, the initial passive and rapid uptake occurs via surface adsorption on the cell wall components, and then subsequent active and slow uptake occurs through the membrane transporting metal ions to the cell.[14] This indicates that cell compositions of algae play a critical role in removing heavy metals from water. Interestingly, the major component of *Undaria pinnatifida* is alginic acid,[15] which is composed of many carboxyl and hydroxyl groups in its chemical structure. Specifically, alginic acid takes account for 20−30% of *U.*

Received: July 8, 2022
Accepted: October 10, 2022
Published: October 24, 2022

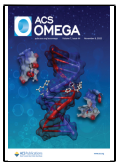

pinnatifida.[16] Particularly, alginic acid is known as soft acid that has a strong affinity for soft ligands that can be utilized for Pb(II) ion removal from water. In this research, we explore the potential of Pb(II) ion removal of *U. pinnatifida* and its characteristics of Pb(II) ion biosorption. Currently, the Pb(II) ion removal kinetics and mechanisms of *U. pinnatifida* have not been systematically investigated yet. Thus, the main objective of this study is to evaluate the biosorption performance of *U. pinnatifida* for the removal of Pb(II) ions from aqueous solutions, as well as to study the underlying biosorption kinetics of *U. pinnatifida* for Pb(II) ion removal.

2. EXPERIMENTAL METHODS

2.1. Chemicals and Materials. All materials were of analytical grade (99%) and purchased from Sigma-Aldrich without further purification.

2.2. Characterization. Fourier transform infrared spectroscopy (FTIR, Shimadzu IR-Tracer 100) with an attenuated total reflectance attachment (ATR, Shimadzu QATR-S; Figure S1) was then used to determine any functional groups (Table S1) within the materials as discussed in the Supporting Information. Images of the adsorbents were obtained by scanning electron microscopy (SEM, JEOL JSM-6060LV). The weight ratio among each element was determined by energy-dispersive X-ray spectroscopy (EDS, Thermo Scientific UltraDry). The elemental 2D mapping images were also obtained by EDS.

2.3. Adsorbent Synthesis. Dry *U. pinnatifida* algae were purchased and then ground into fine powders. These powders were then sieved to obtain a consistent particle size of about 125 μm by passing through a laboratory test sieve. Once these fine algae powders were collected, they were thoroughly cleaned using distilled water and a vacuum filtration system. A side-arm flask was clamped firmly for security along with a Büchner funnel over the opening. A sheet of filter paper was laid on top of the Büchner funnel's porous plate. Once the side-arm flask was connected to the vacuum source using thick-walled tubing, the filter paper was moistened using 2 mL of distilled water. This step was necessary to adhere the paper to the Büchner funnel to avoid the *U. pinnatifida* powder from escaping underneath the filter paper. *U. pinnatifida* was filtered out at a time until all of the powders were rinsed. Finally, the thick-walled tubing was carefully removed from the side-arm flask along with the filter paper.

Since fine *U. pinnatifida* powders can contaminate any given solution, it is required that the algae remain immobilized within alginate beads. The alginate beads were synthesized using 2% sodium alginate and 2.5% calcium chloride with careful control of the size and shape of each bead. The *U. pinnatifida* powders (4 g) were mixed into a 2% sodium alginate solution while stirring using a magnetic stirrer at 60 °C. The 2% sodium alginate solution was created by stirring 2 g sodium alginate in 100 mL of distilled water. Once the mixture became homogenous, a 10 mL syringe was used to form drops of alginate biomass, which were added to a 2.5% calcium chloride solution. The calcium chloride solution was formed by stirring 2.5 g of calcium chloride into 100 mL of distilled water, resulting in immobilized gel-like beads. Distilled water was then used to rinse the immobilized structures twice using vacuum filtration. Once the *U. pinnatifida* algae beads were dried, they were transported to a water filter system to be tested for the removal of Pb(II) ions from wastewater. For comparison, alginate beads were synthesized that contained no marine algae and were also tested for the removal of Pb(II) ions from wastewater.

2.4. Adsorption Study. Once the algae beads were synthesized, we analyzed their Pb(II) ion removal capability. For all Pb(II) ion heavy metal removal trials, Pb(II) ion solutions with a concentration of 100 ppm (parts per million) were prepared by dissolving 1.6 g lead nitrate ($Pb(NO_3)_2$) in 1 L DI water. Standard reaction conditions included 0.6 g of algae beads added to 100 mL of room temperature Pb(II) solution for 24 h unless otherwise specified. Independent experimental parameters include immobilized *U. pinnatifida* beads, solution temperatures ranging from 25 to 40 °C, solution pH, and competing ion concentration. The Pb(II) ion removal capability between powders and beads was compared by adding 30 mg of powder and beads each in 100 mL Pb(II) ion solution (100 ppm) for 1 week to achieve equilibrium adsorption. During the pH trials, the Pb(II) solution pH was altered by adding either nitric acid (HNO_3) or sodium hydroxide (NaOH). The competing ion study was conducted by adding different amounts of potassium nitrate (KNO_3) to the Pb(II) solution. For all trials, the Pb(II) ion levels of the solution were measured by using either inductively coupled plasma atomic emission spectrometry (ICP-AES, Shimadzu ICPE-9810) or a Pb(II) ion test strip.

In particular, the Pb(II) ion removal efficiency was calculated using the following equation

$$\%\ \text{Pb removal efficiency} = \frac{\text{reference ppm} - \text{equilibrium ppm}}{\text{reference ppm}} \times 100 \quad (1)$$

2.5. Adsorption Models. The isotherm study was performed using different amounts of *U. pinnatifida* beads (0.05, 0.11, 0.15, 0.30, 0.60 g) in 100 mL of 100 ppm Pb(II) ion solution. Comparisons with Langmuir and Freundlich isotherm models were made using the following equations. The Langmuir isothermal model is expressed by eq 2[17]

$$Q_e = \frac{X_m K_L C_e}{1 + K_L C_e} \quad (2)$$

where Q_e is the amount (mg) of Pb(II) ion adsorbed per gram of *U. pinnatifida* bead at the equilibrium and C_e (mg/L) is the equilibrium concentration of Pb(II) ions in solution. X_m (mg/g) is the maximum adsorption capacity corresponding to complete monolayer coverage and K_L (L/mg) is a Langmuir constant related to the energy of adsorption. Equation 2 needs to be rearranged to yield the linear form for data extraction

$$\frac{C_e}{Q_e} = \frac{1}{X_m K_L} + \frac{C_e}{X_m} \quad (3)$$

This linear form can be used for linearization of experimental data by plotting C_e/Q_e against C_e and to extract the Langmuir constants X_m and K_L from the slope and intercept of the linear equation. In addition, we used the Freundlich isotherm model that is expressed by eq 4

$$\ln Q_e = \ln k_f + \left(\frac{1}{n}\right) \ln C_e \quad (4)$$

where k_f and n are the Freundlich isotherm constants.

2.6. Temperature Effect. The thermodynamic parameters were measured using 0.6 g of beads and placed in 100 mL of a 100 ppm Pb(II) ion solution for 24 h at temperatures of 25−

https://doi.org/10.1021/acsomega.2c04322
ACS Omega 2022, 7, 39931−39937

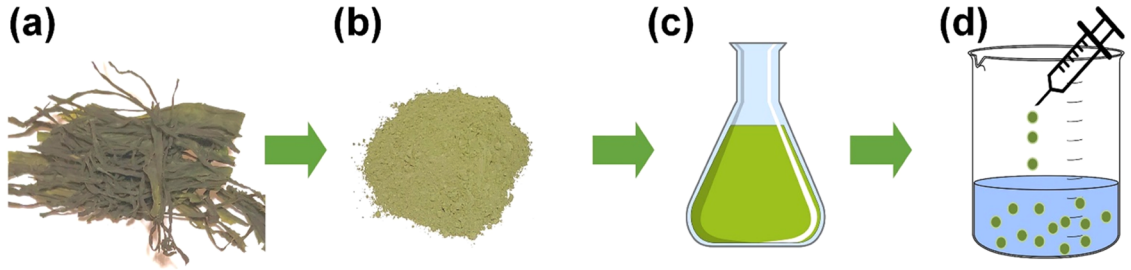

Figure 1. Illustration of immobilization processes by forming beads. (a) Dry, unprocessed pieces of *U. pinnatifida* were purchased. (b) *U. pinnatifida* was ground into ∼125 μm of powder using a 120-mesh sieve. (c) *U. pinnatifida* powder was mixed into a 2% sodium alginate solution. (d) Alginate algae biomass was added dropwise into a calcium chloride solution via a 10 mL syringe, forming beads.

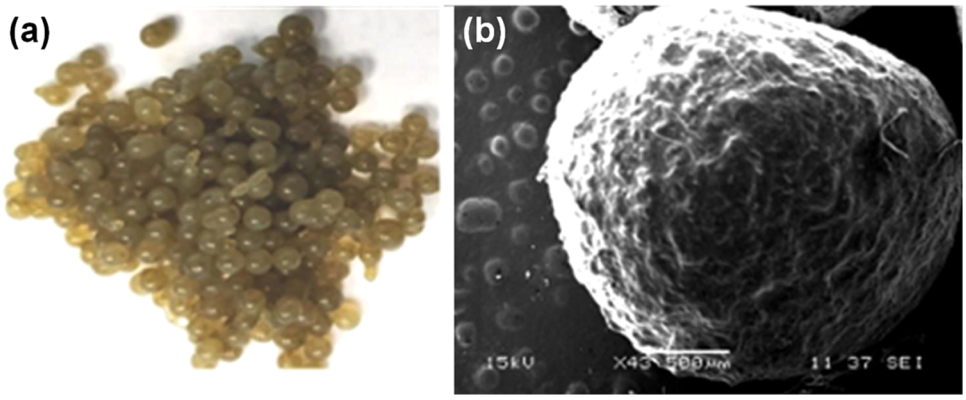

Figure 2. (a) Microscopic image and (b) SEM image of immobilized beads resulting from the immobilization process. SEM image shows a single alginate bead at a scale of 500 μm and a voltage of 15 kV.

40 °C. The values of the equilibrium constant, K_C, for the biosorption of Pb(II) ions from an aqueous solution were calculated as a function of temperature in the 25−40 °C range, using eq 5[18]

$$K_C = \frac{F}{1 - F} \tag{5}$$

where F is the factional attainment of Pb(II) ion biosorption at equilibrium.

Once the equilibrium constant K_C was obtained with temperatures, the thermodynamic quantities, such as ΔG, ΔH, and ΔS, of Pb(II) ion adsorption were calculated using the following equations

$$\Delta G = -RT \ln K_C \tag{6}$$

$$\ln K_C = -\frac{\Delta H}{RT} + \frac{\Delta S}{R} \tag{7}$$

where ΔH = enthalpy, ΔS = entropy, T_k = temperature in Kelvin, and R = universal gas constant (8.131451 J/mol T_k).

3. RESULTS AND DISCUSSION

Figure 1 shows the immobilization process for *U. pinnatifida* powders used to prevent the contamination of solution during Pb(II) ion removal.[19] During this process, calcium ions bind to the sodium alginate strands. Calcium's positive two charge replaces sodium's positive one charge, forcing the calcium ions to create an additional bond to stabilize its electron shell. This creates a firm gel-like membrane allowing the *U. pinnatifida* powder to be immobilized. Once the algae beads were collected, they were thoroughly cleaned using distilled water.

Figure 2a shows the microscopy images of immobilized *U. pinnatifida*, showing sphere beads. The high-resolution SEM image in Figure 2b clearly shows immobilized beads generated from the immobilization process. The spherical bead size was measured to be about ∼2.6 mm and showed a rough surface morphology.

The resulting beads were washed several times with autoclaved distilled water to remove any remains of calcium chloride from the bead surfaces and later stored overnight at 4 °C in distilled water to stabilize and harden the beads. Once immobilized beads are formed, we conducted the Pb(II) ion removal test using beads and powders. For this study, 30 mg of *U. pinnatifida* powders and beads were placed in 100 mL of Pb(II) ion solution (100 ppm) for 1 week to achieve the equilibrium adsorption level at room temperature. After performing Pb(II) ion removal experiments, elemental mapping images using EDS measurement were investigated to determine the biosorption of Pb(II) ions. For this purpose, *U. pinnatifida* beads were dissected after absorbing Pb(II) ions, as shown in Figure S2. The SEM image of the dissected bead is shown in Figure S2a, while Figure S2b−f depicts the distribution of elements (C, O, S, Ca, and Pb). In particular, it is found that lead is uniformly distributed inside the bead after Pb biosorption (Figure S2f), indicating that the immobilized *U. pinnatifida* bead absorbed Pb(II) ions. Figure 3 shows the Pb(II) ion levels from four trial ICP measurements performed on a 100 ppm Pb reference solution, immobilized beads, and powder in Pb(II) ion solution. Table 1 also summarizes the lead level of a reference 100 ppm Pb solution and Pb(II) ion removal test results for *U. pinnatifida* beads and powders. ICP measurement indicates that the reference Pb(II) ion solution showed 100.67 ± 2.65 ppm. *U.*

https://doi.org/10.1021/acsomega.2c04322
ACS Omega 2022, 7, 39931−39937

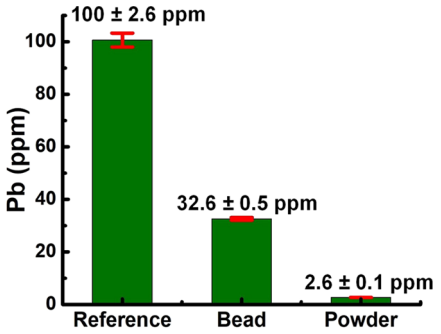

Figure 3. Pb(II) ions removal test results of the 100 ppm Pb reference solution and *U. pinnatifida* beads and powders plotted using data listed in Table 1.

Table 1. Pb(II) Ion Removal Test Results for *U. pinnatifida* Beads and Powders

samples	1st (ppm)	2nd (ppm)	3rd (ppm)	4th (ppm)	average (ppm)
reference	96.76	101.28	102.18	102.46	100.67 ± 2.65
bead	31.86	32.53	33.04	32.93	32.59 ± 0.03
powder	2.67	2.64	2.71	2.69	2.68 ± 0.53

pinnatifida beads partially removed Pb(II) ions from the solution, and the resulting Pb(II) ion level was measured to be 32.6 ± 0.5 ppm, showing ~67.4% removal efficiency. In contrast, *U. pinnatifida* powders removed Pb(II) ions from the solution, and the resulting Pb(II) ion level was measured to be 2.6 ± 0.1 ppm, showing about 97.4% removal efficiency. This clearly indicates that *U. pinnatifida* powders show better Pb(II) ion removal capability compared to *U. pinnatifida* beads. This might be attributed to the fact that *U. pinnatifida* powders use a more active alginic acid surface than *U. pinnatifida* beads because *U. pinnatifida* beads are the mixtures of *U. pinnatifida* and sodium alginate.

Although *U. pinnatifida* powder exhibits better Pb(II) ion removal capacity compared to *U. pinnatifida* beads, the use of *U. pinnatifida* powder may be inefficient to collect the treated *U. pinnatifida* powder from water and may contaminate water as a result. In this regard, it is necessary to effectively utilize the *U. pinnatifida* bead for better Pb(II) ion removal capacity. For this, we further investigated the effects of bead amount and Pb(II) ion solution temperature on Pb(II) ion removal efficiency, as shown in Figure 4a,b, respectively. In this experiment, the Pb(II) ion removal of *U. pinnatifida* beads was tested by varying bead amounts (0.05, 0.11, 0.15, 0.30, 0.60 g) in 100 mL of the 100 ppm Pb(II) ion solution, as shown in Figure 4a. When the amount of beads was increased from 0.05 to 0.3 g in 100 mL of the Pb(II) ion solution, the Pb(II) ion removal rate linearly increased. A further increase in bead amount from 0.3 to 0.6 g in 100 mL of the Pb(II) ion solution led to the almost complete removal of Pb(II) ions. With the bead amount of 0.6 g in 100 mL of the Pb(II) ion solution, Pb(II) ion removal efficiency was measured to be 96.3%. In addition, the temperature of 100 mL of the Pb(II) ion solution (100 ppm) was varied from 25 to 40 °C where 0.3 g of beads were used. As the Pb(II) solution temperature increased from 25 to 40 °C, the Pb(II) ion removal efficiency increased as shown in Figure 4b, indicating that the higher the solution temperature, the better the Pb(II) ion removal efficiency.

To understand the Pb(II) ion removal mechanism of *U. pinnatifida*, isotherm and thermodynamic studies were investigated. For the isothermal study, Langmuir and Freundlich models were the best fitting for lead ion biosorption over *U. pinnatifida* to provide an insight into the biosorption mechanism of Pb(II) ions. Since the Langmuir model explains an adsorbate (in this experiment Pb(II) ions) attached to an adsorbent of *U. pinnatifida* at isothermal conditions, equilibrium conditions were needed where the capacity of the adsorbent material was reached. In this case, different amounts of beads (0.05, 0.11, 0.15, 0.30, 0.60 g) of *U. pinnatifida* beads were placed in 100 mL of the Pb(II) ion solution (100 ppm) for 1 week to achieve the equilibrium adsorption level at room temperature. Then, Pb(II) ion levels were measured and analyzed in terms of Langmuir experimental parameters of C_e and Q_e. Subsequently, the best fitting of the linear form of the Langmuir equation was performed to extract the Langmuir constants X_m and K_L from the slope and intercept of the linear equation. Note that the Langmuir model assumes that adsorption sites on the adsorbent (*U. pinnatifida* bead) surface are occupied by the adsorbate (Pb(II) ions) in the solution. Therefore, the Langmuir constant (K_L) represents the degree of biosorption affinity the adsorbate has to the adsorbent. The X_m value indicates the maximum biosorption capacity associated with complete monolayer coverage that is typically expressed in mg/g. Figure 5a,b shows the best fitting of the linear form $\frac{C_e}{Q_e} = \frac{1}{X_m K_L} + \frac{C_e}{X_m}$ and the original Langmuir isotherm model $Q_e = \frac{X_m K_L C_e}{1 + K_L C_e}$. In contrast, Figure 5c shows the best fitting of the Freundlich isotherm model linear equation

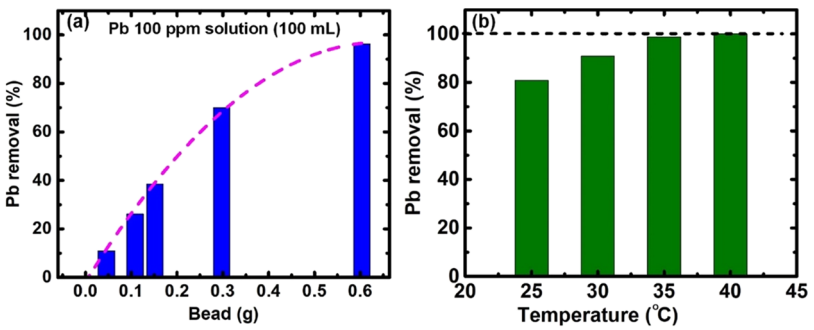

Figure 4. Pb(II) ion removal efficiency as a function of (a) bead amount and (b) Pb(II) ion solution temperature. 0.3 g of beads in 100 mL of Pb(II) ion solution were used for the temperature-dependent ion removal study. Pb removal was determined via ICP analysis with a 1.8% error or less.

https://doi.org/10.1021/acsomega.2c04322
ACS Omega 2022, 7, 39931−39937

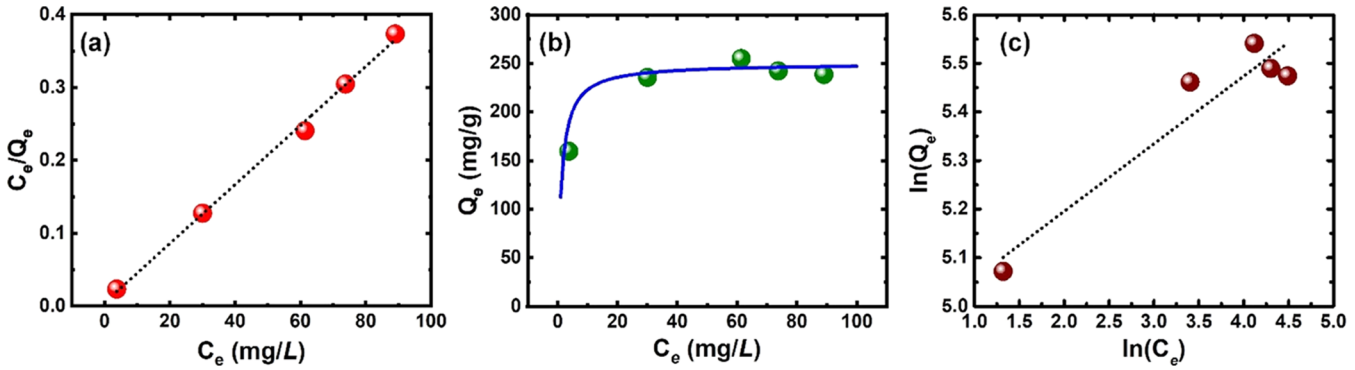

Figure 5. Best fitting of using (a) the linear form for data extraction $\frac{C_e}{Q_e} = \frac{1}{X_m K_L} + \frac{C_e}{X_m}$ and (b) the original Langmuir isotherm model expressed as $Q_e = \frac{X_m K_L C_e}{1 + K_L C_e}$. Using these fittings, the maximum adsorption capacity (X_m) to the complete monolayer coverage Langmuir constant (K_L) was extracted and (c) Freundlich isotherm model linear equation expressed as $\ln Q_e = \ln k_f + \left(\frac{1}{n}\right)\ln C_e$, where k_f and n are the Freundlich isotherm constants.

$\ln Q_e = \ln k_f + \left(\frac{1}{n}\right)\ln C_e$, where k_f and n are the Freundlich isotherm constants. Table 2 also summarizes the Langmuir and Freundlich parameters used to fit the Langmuir and Freundlich equations. Note that when the Langmuir isotherm model was applied, the *R*-squared value was 0.999, which is very close to 1. However, the best fitting of the Freundlich isotherm model has an *R*-squared value of 0.873, as listed in Table 3. This indicates that the Langmuir model accounts for biosorption by *U. pinnatifida* more accurately than the Freundlich isotherm model. From the Langmuir isotherm model, we extracted the maximum adsorption capacity (X_m) to the complete monolayer coverage Langmuir constant (K_L). It is found that the X_m of *U. pinnatifida* for Pb(II) ions was 250.00 mg/g and the Langmuir constant (K_L) was 0.816 L/mg, as listed in Table 2. Note that from our best fitting of Langmuir in Figure 5, the X_m of *U. pinnatifida* was 250.00 mg/g, which is almost 5 times larger than that (54.95 mg/g) of activated carbon for Pb(II) ions.[18] This indicates that the Pb(II) ion removal capability of *U. pinnatifida* is superior to that of activated carbon. In addition, it is found that Langmuir constant values, K_L, of *U. pinnatifida* and activated carbon for Pb(II) ions were similar.

Table 2. Summary of the Batch Biosorption Test Result for Pb(II) Ions

samples	C_e(mg/L)	Q_e(mg/g of bead)	C_e/Q_e	In(C_e)	ln(Q_e)
1	89.05	238.45	0.37	4.49	5.47
2	73.79	242.18	0.31	4.30	5.49
3	61.38	254.92	0.24	4.12	5.54
4	30.02	235.45	0.13	3.40	5.46
5	3.74	159.50	0.02	1.32	5.07

Table 3. Linear Regression Data for Langmuir and Freundlich Isotherms

	Langmuir model			Freundlich model		
adsorbent	K_L (L/mg)	X_m (mg/g)	R^2	K_f	n	R^2
U. pinnatifida	0.816	250.00	0.990	66.14	7.19	0.873
activated carbon[a]	0.938	54.95	0.996	[b]	[b]	[b]

[a]Activated carbon data taken from ref 18. [b]Not reported.

To further explore the underlying thermodynamic kinetics on the biosorption of *U. pinnatifida* beads, thermodynamic quantities such as Gibbs free energy (ΔG), enthalpy (ΔH), and entropy (ΔS) values of Pb(II) ion biosorption of *U. pinnatifida* were analyzed. Figure 6 shows the equilibrium constant (K_C) values as a function of Pb(II) ion solution temperature in the form of $1/T$ in Kelvin. This clearly shows that K_C values increased with increased Pb(II) ion solution temperatures. The resultant thermodynamic quantities (ΔG, ΔH, and ΔS) of Pb ion biosorption are listed in Table 4. These values were calculated from the K_C values using the equations $\Delta G = -RT\ln K_C$, $\ln K_C = -\frac{\Delta H}{RT} + \frac{\Delta S}{R}$ where ΔH = enthalpy, ΔS = entropy, T_k = temperature in Kelvin, and R = universal gas constant (8.131451 J/mol T_k). The equilibrium values of ΔG, ΔH, and ΔS for *U. pinnatifida* are presented in Table 4. Interestingly, values of ΔG became more negative with increased temperatures from −3.48 kJ/mol at 25 °C to −10.96 kJ/mol at 35 °C. The large negative values of ΔG for *U. pinnatifida* indicate that the reactions are strongly spontaneous. This indicates that an increase in Pb(II) ion solution temperature offers a more preferential reaction toward

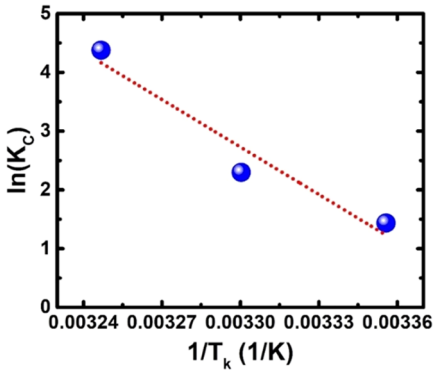

Figure 6. Equilibrium constant, K_C for the adsorption of Pb ions from aqueous solution calculated as a function of temperature in the 25−40 °C range, using the equation $K_C = \frac{F}{1-F}$ where F is the factional attainment of Pb(II) ion adsorption at equilibrium.

https://doi.org/10.1021/acsomega.2c04322
ACS Omega 2022, 7, 39931−39937

Table 4. Calculated Thermodynamic Quantities of Pb(II) Ion Biosorption

K_C (dimensionless)			ΔG(kJ/mol)				
25 °C	30 °C	35 °C	25 °C	30 °C	35 °C	ΔH(kJ/mol)	ΔS(kJ/mol)
4.21	9.95	79.65	−3.48	−5.66	−10.96	218.94 ± 54.6	0.74 ± 0.18

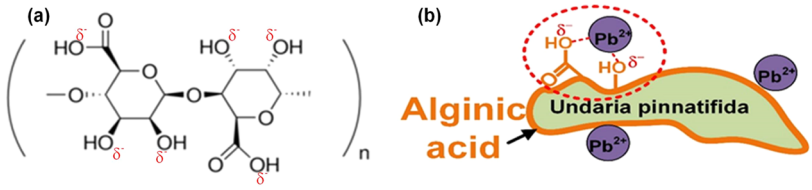

Figure 7. (a) Structure of alginic acid composed of carboxyl and hydroxyl groups and (b) biosorption mechanism of Pb(II) ions where *U. pinnatifida* is covered with alginic acid, in which negatively charged hydroxyl radicals (OH) promoted the biosorption of Pb(II) ions.

Pb(II) ion biosorption. In addition, the extracted ΔH value was positive, inferring that biosorption processes were found to be endothermic and a temperature increase aided the Pb(II) ion biosorption process (i.e., positive change in enthalpy (ΔH)) through the activation of biosorption sites. Generally, this might be due to the fact that an increase in Pb(II) ion solution temperature aided the biosorption process through activation of biosorption sites.

When the adsorption ability of *U. pinnatifida* was tested at different pH values ranging from 2 to 12 (Figure S3), it was found that the ideal pH conditions for *U. pinnatifida* facilitated Pb(II) ion removal were pH 3−5. As shown in Figure S3, there was a sharp increase in Pb(II) ion adsorption at pH values greater than 5.0. This increased adsorption may be due to the chemical precipitation of lead ions as lead hydroxide ($Pb(OH_2)$) rather than adsorption by the algae beads.[18] At lower pH values, the adsorption of lead ions appears to decrease, possibly due to the competition for adsorption sites between hydrogen ions [H^+] or hydronium ions [H_3O^+] with Pb^{2+} ions. In addition, it is found that increasing the concentration of KNO_3 (i.e., increasing the ionic strength) in solution (Figure S4) also caused an increase in Pb(II) ion adsorption. Previous literature for lead and other metal ion adsorption has also reported an enhanced adsorption ability by increasing the ionic strength.[18−20,22,23] It is theorized that the presence of K^+ ions causes the surface potential of *U. pinnatifida* to become more negative. This occurs via the hydrolysis of surface −OH and −COOH functional groups (Figure 7a) to $-O^-$ and $-COO^-$ (Figure 7b), which attract more Pb^{2+} ions.[18,20,21] The reaction rate of the Pb(II) ion adsorption by *U. pinnatifida* was determined to be $1.4 \times 10^{-3} k_1$ (min^{-1}) (Table S2) and followed first-order reaction kinetics (Figure S5).

Based on quantitative and qualitative analyses, we modeled the Pb(II) biosorption mechanism using *U. pinnatifida*, as shown in Figure 7. *U. pinnatifida* contains a high level of alginic acid that accounts for 20−30%.[16] As shown in Figure 7a,b, alginic acid is composed of many carboxyl and hydroxyl groups in which negatively charged hydroxyl radicals (OH) can promote the biosorption of Pb(II) ions. However, our initial test of Pb(II) ion removal via unprocessed *U. pinnatifida* did not show significant Pb(II) ion removal. This indicates that alginic acid was not properly activated in a way to efficiently uptake Pb(II) ions from water by increasing available biosorption sites on the *U. pinnatifida* surface, which can promote the Pb(II) ion biosorption. To remedy this problem, *U. pinnatifida* was ground into micron-size *U. pinnatifida* powders (Figure 1). Remarkably, even a small amount (30 mg in 100 mL of Pb(II) ion solution) of *U. pinnatifida* powder showed a removal efficiency of 97.4%. Even with high Pb(II) ion removal efficiency, we encountered water contamination problems due to fine powders that can be dispersed in water and cannot be completely collected from water. To avoid this issue, *U. pinnatifida* powders were immobilized in beads with an average diameter of 2.6 mm.

4. CONCLUSIONS

This study focused on investigating the Pb(II) ion removal using algae beads made from *U. pinnatifida*. Various quantitative studies were performed and the remaining Pb(II) ion concentration was measured using ICP-AES. Our findings are as follows:

(1) When the Pb(II) ion solution temperature increases, a higher Pb(II) ion removal efficiency of *U. pinnatifida* was observed.
(2) The Pb(II) ion removal from water can be enhanced by increasing ionic strength, likely because the added K^+ cations hydrolyze the hydroxyl and carboxyl groups. This created a more negative surface area to attract Pb(II) ions.
(3) The adsorption data fit first-order kinetics and the Langmuir adsorption model. The calculated adsorption capacity of *U. pinnatifida* for Pb(II) ion removal is ∼5 times more efficient than activated carbon's Pb(II) ion removal capabilities.

Current research focuses on *U. pinnatifida*-based Pb(II) ion removal from water. However, we believe that the current experimental design could be expanded to further discover methods for absorbing other heavy metals such as Cd, Pb, Ni, etc. Newly explored Pb(II) ion removal strategies using an inexpensive yet efficient *U. pinnatifida* system can be further developed to replace expensive home filter systems. In addition, *U. pinnatifida* can be used as a potential candidate for environment-friendly, economical, and easily available waste-removing agents in industrial effluents and municipal wastewater.

■ ASSOCIATED CONTENT

Supporting Information

The Supporting Information is available free of charge at https://pubs.acs.org/doi/10.1021/acsomega.2c04322.

FTIR analysis of *U. pinnatifida* powder and beads before and after lead adsorption (Figure S1); observed peaks

https://doi.org/10.1021/acsomega.2c04322
ACS Omega 2022, 7, 39931−39937

and their associated functional groups (Table S1); elemental mapping of bisected algae bead after a 24 h Pb(II) adsorption for C, O, S, Ca, and Pb (Figure S2); equilibrium adsorption capacity (Q_e (mg/g)) versus solution pH ranging from pH 2 to 12 (Figure S3); equilibrium adsorption capacity Q_e (mg/g) versus competing ion (KNO_3) concentration (M) (Figure S4); reaction order graphs for zero order, first order, and second order reactions (Figure S5); and kinetic model parameters for lead ion adsorption via a biosorbent (Table S2) (PDF)

AUTHOR INFORMATION

Corresponding Author

Tarek M. Abdel-Fattah − *Applied Research Center at Thomas Jefferson National Accelerator Facility and Department of Molecular Biology and Chemistry at Christopher, Newport University, Newport News, Virginia 23606, United States;* orcid.org/0000-0003-1454-7421; Email: fattah@cnu.edu

Authors

Hannah Namkoong − *Applied Research Center at Thomas Jefferson National Accelerator Facility and Department of Molecular Biology and Chemistry at Christopher, Newport University, Newport News, Virginia 23606, United States; Department of Chemical and Biomolecular Engineering, Johns Hopkins University, Baltimore, Maryland 21218, United States*

Erik Biehler − *Applied Research Center at Thomas Jefferson National Accelerator Facility and Department of Molecular Biology and Chemistry at Christopher, Newport University, Newport News, Virginia 23606, United States*

Gon Namkoong − *Department of Electrical and Computer Engineering, Applied Research Centre, Old Dominion University, Newport News, Virginia 23606, United States;* orcid.org/0000-0002-9795-8981

Complete contact information is available at: https://pubs.acs.org/10.1021/acsomega.2c04322

Notes

The authors declare no competing financial interest.

ACKNOWLEDGMENTS

T.M.A.-F. acknowledges Lawrence J. Sacks Professorship in Chemistry.

REFERENCES

(1) Jaishankar, M.; Tseten, T.; Anbalagan, N.; Mathew, B. B.; Beeregowda, K. N. Toxicity, mechanism and health effects of some heavy metals. *Interdiscip Toxicol.* **2014**, *7*, 60−72.

(2) Thurmer, K.; Williams, E.; Reutt-Robey, J. Autocatalytic oxidation of lead crystallite surfaces. *Science* **2002**, *297*, 2033−2035.

(3) Bishop, B. E.; Savitzky, B. A.; Abdel-Fattah, T. M. Lead bioaccumulation in emydid turtles of an urban lake and its relationship to shell disease. *Ecotoxicol. Environ. Saf.* **2010**, *73*, 565−571.

(4) Lo, W.; Chua, H.; Lam, K. H.; Bi, S. P. A comparative investigation on the biosorption of lead by filamentous fungal biomass. *Chemosphere* **1999**, *39*, 2723−2736.

(5) Esalah, J. O.; Weber, M. E.; Vera; J, H. Removal of lead, cadmium and zinc from aqueous solutions by precipitation with sodium Di-(*n*-octyl) phosphinate. *Can. J. Chem. Eng.* **2000**, *78*, 948−954.

(6) Gupta, K. V.; Gupta, M.; Sharma, S. Process development for the removal of lead and chromium from aqueous solutions using red mud-an aluminum industry waste. *Water Res.* **2001**, *35*, 1125−1134.

(7) Esalah, J. O.; Weber, M. E.; Vera, J. H. Removal of lead, cadmium and zinc from aqueous solutions by precipitationwith sodium di-(n-octyl) phosphinate. *Can. J. Chem. Eng.* **2000**, *78*, 948−954.

(8) Kang, K. C.; Kim, S. S.; Choi, J. W.; Kwon, S. H. Sorption of Cu2+ and Cd2+ onto acid and base pretreated granular activated carbon and activated carbon fiber samples. *J. Ind. Eng. Chem.* **2008**, *14*, 131−135.

(9) Arief, V. O.; Trilestari, K.; Sunarso, J.; Indraswati, N.; Ismadji, S. Recent Progress on biosorption of heavy metals from liquids using low cost biosorbents: Characterization, biosorption parameters and mechanism studies. *Clean Soil, Air, Water* **2008**, *36*, 937−962.

(10) Gunasundari, D.; Muthukumar, K. Simultaneous Cr (VI) reduction and phenol degradation using *Stenotrophomonas* sp. Isolated from tannery effluent contaminated soil. *Environ. Sci. Pollut. Res.* **2013**, *20*, 6563−6573.

(11) Wilde, E. W.; Benemann, J. R. Bioremoval of heavy metals by the use of microalgae. *Biotechnol. Adv.* **1993**, *11*, 781−812.

(12) Tüzün, İ.; Bayramoğlu, G.; Yalçin, E.; Başaran, G.; Celik, G.; Arica, M. Y. Equilibrium and kinetic studies on biosorption of Hg(II), Cd(II) and Pb(II) ions onto microalgae *Chlamydomonas reinhardtii*. *J. Environ. Manage* **2005**, *77*, 85−92.

(13) Herrero, R.; Lodeiro, P.; Rojo, R.; Ciorba, A.; Rodri'guez, P.; Sastre de Vicente, M. E. The efficiency of the red alga *Mastocarpus stellatus* for remediation of cadmium pollution. *Bioresour. Technol.* **2008**, *99*, 4138−4146.

(14) Vymazal, J. Uptake of lead, chromium, cadmium and cobalt by *Cladophora glomerate*. *Bull. Environ. Contam. Toxicol.* **1990**, *44*, 468−472.

(15) Kim, Y. H.; Park, J. Y.; Yoo, Y. J.; Kwak, J. W. Removal of lead using xanthated marine brown alga, *Undaria pinnatifida*. *Process Biochem.* **1999**, *34*, 647−652.

(16) Lee, Y. J. A Study on Mineral and Alginic acid Contents by Different Parts of Sea Mustards (*Undaria pinnatifida*). *J. Korean Soc. Food Cult.* **2004**, *19*, 691−700.

(17) Langmuir, I. The constitution and fundamental properties of solids and liquids. Part I: Solids. *J. Am. Chem. Soc.* **1916**, *38*, 2221−2295.

(18) Payne, K. B.; Abdel-Fattah, T. M. Adsorption of Divalent Lead Ions By Zeolites and Activated Carbon: Effects of PH, Temperature, and Ionic Strength. *J. Environ. Sci. Health* **2004**, *39*, 2275−2291.

(19) Abdel-Fattah, T. M.; Mahmoud, M. E. Selective extraction of toxic heavy metal oxyanions and cations by a novel silica gel phase functionalized by vitamin B4. *Chem. Eng. J.* **2011**, *172*, 177−183.

(20) Abdel-Fattah, T. M.; Mahmoud, M. E. Heavy metal ions extraction from aqueous media using nanoporous silica. *Chem. Eng. J.* **2011**, *171*, 177−183.

(21) El-Naggar, N.-A.; Hamouda, R. A.; Mousa, I. E.; Abdel-Hamid, M. S.; Rabei, N. H. Statistical optimization for cadmium removal using Ulva fasciata biomass: Characterization, immobilization and application for almost-complete cadmium removal from aqueous solutions. *Sci. Rep.* **2018**, *8*, No. 12456.

(22) Bolan, N. S.; Syers, J. K.; Tillman, R. W. Ionic strength effects on surface charge and adsorption of phosphate and sulphate by soils. *Eur. J. Soil Sci.* **1986**, *37*, 379−388.

(23) Wang, Y.; Huang, H.Carbon Nanotube Composite Membranes for Microfiltration of Pharmaceuticals and Personal Care Products. In *Macro & Nano Technologies*; Elsevier B.V., 2019; Chapter 8, pp 183−202.